DETERMINATION OF DRYING BEHAVIOUR IN INDUSTRIAL TYPE CONVECTIONAL DRYER AND MATHEMATICAL MODELLING

by

Ahmet Erhan AKAN[a*] and Derya Burcu OZKAN[b]

[a] Corlu Vocational School, Department of Machinery, Namik Kemal University, Tekirdag, Turkey
[b] Mechanical Engineering Department, Yildiz Teknik University, Istanbul, Turkey

Original scientific paper
https://doi.org/10.2298/TSCI180315244A

In this study, the performance of a stenter (ram machine) that enables the drying of textile products with hot air is theoretically modelled with a diffusion model derived from Fick's second law. The experimental study was conducted in a 10 chamber stenter with three different drying temperatures (110-130-150 °C) and three different fabric speeds (10-20-30 m per minute.) by using a fabric consisting of 95% cotton + 5% lycra. The drying behaviour of the dryer was determined by utilizing the data obtained from the studies. With the help of the utilized model, the values of diffusion coefficients and activation energies were obtained, the conformity of data between the model and the experimental studies were compared by using regression analysis, it was observed that the R^2 *value varied between 0.9812 and 0.9961.*

Key words: *drying, mathematical modelling, stenter, diffusion model, heat and mass transfer*

Introduction

In order to obtain processes that use energy more efficiently, it is very important to develop drying processes that will minimize the duration of drying with minimum energy consumption without deteriorating the quality and structure of the material, and to improve drying methods in this regard [1].

Stenters (ram machines) are the most widely used convection drying machines in the textile industry that do not damage the structure of the product during drying as well as being able to adjust the desired width/length ratio. Stenters are drying machines in which fabrics are fixed inside the machine in a horizontal way by means of pallets and the movement of the fabric is enabled through chains while hot air is blown [2]. There are various conducted studies in the literature regarding the mathematical modelling of textile drying processes. According to the conducted studies;

Baxi *et al.* [3] modified the semi-empirical model based on mass and moisture balancing equations between vegetables and drying air in a MATLAB-Simulink environment for rotary type dryers and developed it. They then compared these with stenters [3]. Ghali *et al.*, [4] presented a numerical model in order to simulate the heat and mass transfer during the drying process of fabrics. The model was applied on two different types of fabric, cotton and polypropylene. The model they developed shows that water creates two different heat regions when passing through fabric samples. Sousa *et al.*, [5] aimed to determine the drying charac-

* Corresponding author, e-mail: aeakan@nku.edu.tr

teristics of the raw cotton fabric drying process with two different perspectives. They proved that a higher evaporation rate could be achieved resulting in decreased drying time through increasing the drying temperature by controlling the heat and mass transfer in the drying process. Park and Baik [6] analysed the heat and mass transfer of a fabric dried in a ram machine. They have solved the temperature and moisture content distribution by using the finite elements method. They also explained the effects of operating parameters such as moisture, temperature and initial temperature alongside heat and mass transfer coefficients of the fabric in the stenter. Etemoglu *et al.* [7] conducted a theoretical and experimental analysis of drying fabric over a constantly moving straight layer. They developed a mathematical model for heat and mass transfer analysis of fabric in a ram air jet dryer. In the model, they acknowledged that the fabric has a porous medium while the duration of drying, and the vapour pressure of the liquid evaporated on the drying surface remained at a nearly saturated value corresponding to the temperature of the liquid. Johann *et al.* [8] developed a model that reflected the convective drying processes of textile materials. For the mathematical modelling, they made use of mass and energy balances using the finite differences method in Cartesian co-ordinates. They stated that the R^2 value of the model they obtained in statistical analysis by using the Shapiro-Wilk test was over 0.997. Alnak and Karabulut [9] investigated the heat and mass transfer in the jet drying by using moist objects which have different geometric shapes of straight and reverse semi-circular. In the calculations performed with four different Reynolds numbers, they used the finite volume method to solve momentum and energy equations. As a result, they found that increasing values of the number of Reynolds showed a favourable effect on heat and mass transfer.

Material and method

Experimental set-up

The experimental study was carried out in a 10 chamber stenter, figs. 1 and 2, installed in a textile manufacturing plant. Fabrics preferred in the experiments were the fabrics used in the production process of the enterprise and the obtained results consist of data from actual production conditions. In the stenter, each chamber consisted of one 350 kW automatically controlled burner and four 4 kW cross positioned automatically controlled fans. The chambers have a length of 3 m and the drying air temperature can be adjusted between 100-200 °C.

Figure 1. A photo related to stenter overview

Figure 2. A photo related to foulard section and mechanical drying

Properties of the fabric used in the studies

The fabric used in the studies is a fabric of 95% cotton and 5% lycra with a 30/1 compact supreme lattice structure. After being kept in the drying oven for 24 hours under standard atmospheric conditions (20 °C, 65% RH), 5 samples of 100 cm^2 were taken and weighed with a precision scale and the dry weight of the fabric was found to be 133 g/m^2 after taking their arithmetic average. The thickness of the fabric was determined to be 0.77 mm.

Experimental procedure and data obtained

Before being taken to the drying chambers, fabrics used in the studies were subjected to a pre-drying process between the wringers after the washing operation in the foulard section. The RH and surface temperature of the pre-dried fabric, before being sent to the first chamber, was measured to be 60% and 35°, respectively. The studies were conducted in three different drying air temperatures as 110, 130, and 150 °C and three different fabric speeds as 0.167, 0.333, and 0.500 m/s. It was determined that the temperature and RH of the environment in which the studies were conducted were 27.6 °C and 60%, respectively. The exit velocity and flow rate of the drying air coming out from the air outlets found on the eight pairs of nozzles in each chamber were measured. Accordingly, the average air speed and flow-rate for drying air of 110 °C was found to be 21.85 m/s and 0.194 kg/s, for drying air of 130 °C the air speed was 24.45 m/s and flow-rate was 0.206 kg/s, whereas for drying air of 150 °C the air speed was 33.4 m/s and the flow-rate was 0.268 kg/s. The surface temperatures of the fabric in the chamber entry and exit points during the drying process as well as the RH and temperature in the boundary layer were measured by using the measurement devices provided in tab. 4, figs. 3 and 4, and the obtained values are shown in tabs. 1-3. At the end of the drying process, the relative humidity values of the fabric released from the dryer were measured with the help of fabric RH measurement device and experimental moisture loss of the fabric was obtained. These values have compared with the moisture loss values obtained as a result of calculations and they are presented in tab. 5.

Method

The assumptions made in the calculations

– It has been assumed that the liquid properties are stable, the porous medium is saturated, and that the dryer is adiabatic.

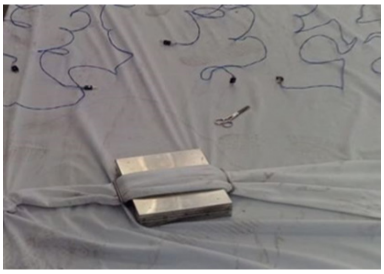

Figure 3. Placement of probes on the fabric

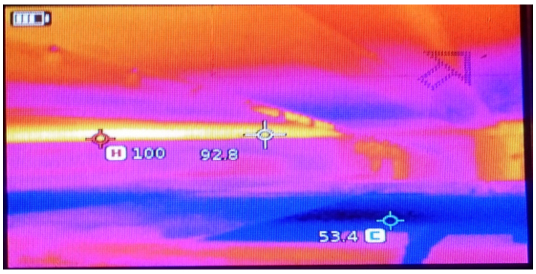

Figure 4. Thermal camera view of fabric inside the chamber

Table 1. Experimental data obtained at feed rate of 0.167 m/s

Fabric velocity [ms^{-1}]	Drying air temperature		110 °C			130 °C			150 °C		
	Chamber	Time [s]	Fabric surface temperature [°C]	Moist air relative humidity [% RH]	Moist air temperature [°C]	Fabric surface temperature [°C]	Moist air relative humidity [% RH]	Moist air temperature [°C]	Fabric surface temperature [°C]	Moist air relative humidity [% RH]	Moist air temperature [°C]
0.167	Inlet	–	35	–	–	35	–	–	35	–	–
	1. Chamber	18	58	66,3	57	74	68.3	56	74	72	52
	2. Chamber	36	70	49.6	59	84	51	58	82	54.5	53
	3. Chamber	54	85	36.3	62	110	37	61	112	41.7	55
	4. Chamber	72	91	26.2	65	118	27.6	63	120	30	58
	5. Chamber	90	96	16.6.	71	122	18.1	68	132	21.2	61
	6. Chamber	108	100	12.3	73	122	13.6	70	139	15	65
	7. Chamber	126	102	8.2	79	123	9.6	74	142	10.8	69
	8. Chamber	144	102	7.2	81	124	8.1	77	143	8.7	73
	9. Chamber	162	103	6.4	83	125	7	79	144	7.6	75
	10. Chamber	180	100	6.3	82	119	6.9	79	142	7	76
	Outlet	–	68	–	–	93	–	–	111	–	–

Table 2. Experimental data obtained at feed rate of 0.333 m/s

Fabric velocity [ms^{-1}]	Drying air temperature		110 °C			130 °C			150 °C		
	Chamber	Time [s]	Fabric surface temperature [°C]	Moist air relative humidity [% RH]	Moist air temperature [°C]	Fabric surface temperature [°C]	Moist air relative humidity [% RH]	Moist air temperature [°C]	Fabric surface temperature [°C]	Moist air relative humidity [% RH]	Moist air temperature [°C]
0.333	Inlet	–	35	–	–	35	–	–	35	–	–
	1. Chamber	9	58	60.4	70	67	62.2	69	73	67.2	64
	2. Chamber	18	67	45	72	78	46.3	71	79	48.1	66
	3. Chamber	27	71	32.5	75	82	33	74	84	34.8	69
	4. Chamber	36	77	23.8	77	96	25.5	5	93	26.6	69
	5. Chamber	45	84	15.1	82	107	16.5	79	125	18.9	72
	6. Chamber	54	86	11.6	83	111	12.8.	80	133	13.4	75
	7. Chamber	63	98	7.9	88	116	8.9	84	138	10.2	77
	8. Chamber	72	102	6.9	90	120	7.3	87	141	8.5	80
	9. Chamber	81	103	6.4	91	124	6	90	142	7	83
	10.Chamber	90	102	6.2	91	119	5.7	91	135	5.8	86
	Outlet	–	85	–	–	100	–	–	113	–	–

Table 3. Experimental data obtained at feed rate of 0.500 m/s

Fabric velocity [ms^{-1}]	Drying air temperature		110 °C			130 °C			150 °C		
	Chamber	Time [s]	Fabric surface temperature [°C]	Moist air relative humidity [% RH]	Moist air temperature [°C]	Fabric surface temperature [°C]	Moist air relative humidity [% RH]	Moist air temperature [°C]	Fabric surface temperature [°C]	Moist air relative humidity [% RH]	Moist air temperature [°C]
0.500	Inlet	–	35	–	–	35	–	–	35	–	–
	1. Chamber	6	56	56.8	78	64	58.5	77	72	62.9	72
	2. Chamber	12	65	44.1.	79	72	45.7	78	76	45.6	74
	3. Chamber	18	68	30.6	83	77	32.9	80	80	34.1	75
	4. Chamber	24	72	21.3	86	88	21.6	85	87	23.1	77
	5. Chamber	30	81	14.4	90	97	14.6	88	103	16.5	80
	6. Chamber	36	86	10.2	93	105	10.9	90	118	11.5	84
	7. Chamber	42	96	6.9	99	113	8.1	93	128	9.4	85
	8. Chamber	48	102	6.1	100	118	6.5	97	140	7.4	89
	9. Chamber	54	103	5.7	101	123	5.5	100	141	6.5	91
	10.Chamber	60	94	5.5	101	115	5.1	102	132	5.2	95
	Outlet	–	89	–	–	112	–	–	120	–	–

– As the drying air coming into contact with the fabric is constantly renewed, the moisture and temperature of the drying air were not affected by the temperature and moisture change in the fabric.
– It has been assumed that the porous material is homogeneous and rigid and that the fabric moving in the dryer is considered as a flat plate.
– Simultaneous heat and mass transfer have been considered in the calculations.

Table 4. Measurement devices and sensitivity

Measurement device	Sensitivity
Testo 350M/XL, Portable gas analyser (Air velocity measurement)	5%
Testo 870-2 thermal camera	±2% °C
Hygro Faster Ekv (Fabric moisture measurement)	0.8%
Delta Ohm HD 2301 (Air moisture measurement)	±0.1%*RH*
Digitron ThermaPro 2 data logger (*K*-type probe, Fabric surface temperature)	0.5%
Desis THB 600 Precision scales	0.01g

Table 5. Fabric relative humidity values at dryer inlet and outlet

Drying air temperature	Fabric speed [ms^{-1}]	Fabric inlet relative humidity [%]	Experimental fabric outlet relative avg. humidity [%]	Theoretical fabric outlet relative avg. humidity [%]
110 °C	0.167	60	6.42	6.20
	0.333	60	10.85	10.40
	0.500	60	13.35	13.00
130 °C	0.167	60	4.96	4.70
	0.333	60	8.62	8.30
	0.500	60	10.95	11.30
150 °C	0.167	60	3.27	3.00
	0.333	60	5.96	5.80
	0.500	60	9.30	9.90

Heat and mass transfer

A drying process is an event consisting of simultaneous heat and mass transfer and solving such problems requires the consideration of simultaneous heat and mass transfers [10]. As this study consists of drying under high-speed ramjets, the Chilton-Colburn similarity eq. (1), (Pr ≠ Sc ≠ 1) has been used:

$$h = \rho c_p h_m \,\mathrm{Le}^{2/3} \tag{1}$$

The temperature of the film that is created during the drying process between the drying air and the fabric was determined using eq. (2) and dimensionless numbers were reached by using the thermodynamic properties (ρ, C_p, k, α, D_{AB}, μ, ν, Pr) of air at this temperature. Thermodynamic properties of air at film temperature are given in *Appendix 1*:

$$T_\mathrm{f} = \frac{T_\mathrm{da} + T_\mathrm{fs}}{2} \tag{2}$$

In determining the flow type, Reynolds number was analyzed on the straight plate eq. (3). Calculated Reynolds numbers are higher than the critical value and flow over the entire plate was considered as turbulent:

$$\mathrm{Re} = \frac{VL_c}{\nu} > 5\cdot 10^5 \tag{3}$$

Developed average Nusselt and Sherwood numbers regarding turbulent flow for forced external convection over a straight plate ($5\cdot 10^5 < \mathrm{Re} < 10^7$) as well as heat and mass convection coefficients were determined from eqs. (4) and (5):

$$\mathrm{Nu} = 0.037\,\mathrm{Re}_\mathrm{L}^{0.8}\,\mathrm{Pr}^{1/3} = \frac{hL}{k} \tag{4}$$

$$\mathrm{Sh} = 0.037\,\mathrm{Re}_\mathrm{L}^{0.8}\,\mathrm{Sc}^{1/3} = \frac{h_m L}{D_{AB}} \tag{5}$$

Determination of theoretical evaporation amount

There are a total of eight pairs (bottom + top) of nozzle series which consists of 105 nozzles (∅ = 7 mm), fig. 5, in each chamber. The amount of moisture removed from the fabric is calculated by assuming it is equal to the amount of moisture that can be removed by the dry air blown on to the fabric from the nozzles for the duration in which the fabric remained within the chambers. Therefore the drying air-flow rate for each nozzle series is calculated and the evaporation amount was determined by using moist air specific humidity and drying air specific humidity values eqs. (6)-(8). Additionally, in the fig. 6, schematic representation of measuring points of nozzles in each chamber is presented.

Figure 5. Location of nozzle series

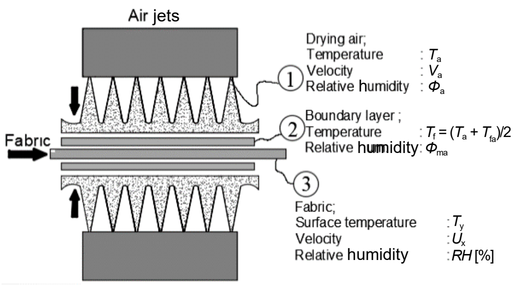

Figure 6. Schematic representation of measuring points of nozzles in each chamber

– Drying air-flow rate for a single nozzle:

$$\dot{m}_\mathrm{a,single} = \rho V A_\mathrm{nozzle} \tag{6}$$

– Drying air-flow rate for nozzle series:

$$\dot{m}_\mathrm{series} = 210\dot{m}_\mathrm{a,single} \tag{7}$$

– Evaporation amount:

$$M_\mathrm{e} = \dot{m}_\mathrm{a,series}(\omega_\mathrm{moist\ air} - \omega_\mathrm{drying\ air})t \tag{8}$$

Determination of drying behaviour

The humidity of a wet material is the ratio of the moisture mass within the material to the total mass of the material and is called the wet basis moisture content [1]:

$$X_{\mathrm{w}} = \frac{m_m}{m_d} \tag{9}$$

where X_{w} [kg moisture(kg wet material)$^{-1}$] is the wet basis moisture content of the material, m_{w} [kg] – the water mass within the material, m_{d} [kg] – the mass of the wet material.

The drying rate expresses the amount of moisture being removed from the fabric within a duration of Δt, and is calculated by the following formula [11]:

$$\frac{\Delta M}{\Delta t} = \lim_{\Delta t \to 0} \frac{M_{t+\Delta t} - M_t}{\Delta_t} \tag{10}$$

Here, $\Delta M / \Delta t$ [kg water (kg dry material × second)$^{-1}$], expresses the drying rate, $M_{t+\Delta}$ [kg water(kg dry material)$^{-1}$] expresses the moisture content at time $t+\Delta t$, M_t [kg water(kg dry material)$^{-1}$] expresses the moisture content at time t, and Δt [s] express time.

Modelling

The diffusion model was used in the determination of drying behaviour. In this model, it is assumed that the removable moisture found within the material to be dried is transferred to the surface through diffusion and that it dissipates from the surface in a vapour state after interacting with the air. In the model, it is assumed that the effects of other drying mechanism are within the diffusion coefficient. Thus the diffusion coefficient in the model takes the form of an effective diffusion coefficient [12]. The diffusion model is based on the solution of Fick's 2$^{\text{nd}}$ law. The isotropic diffusion in the 1-D mass transfer during the drying of different materials is expressed through Fick's 2$^{\text{nd}}$ law as given [13]:

$$\frac{\partial M}{\partial t} = D_{\mathrm{eff}} \left(\frac{\partial^2 M}{\partial x^2} + \frac{k \partial M}{x \partial x} \right) \tag{11}$$

where M is moisture content, t [s] – the time, D_{eff} [m^{2}s^{-1}] – the effective diffusion coefficient, for flat plates $k = 0$, for cylinders $k = 1$ and for spheres $k = 2$ [14]:

$$MR = \frac{M - M_{\mathrm{e}}}{M_0 - M_{\mathrm{e}}} = \frac{8}{\pi^2} \sum_{n=1}^{\infty} \frac{1}{(2n-1)} \exp\left[-\frac{(2n-1)^2 \pi^2 D_{\mathrm{eff}}\, t}{4L^2} \right] \tag{12}$$

Here, MR is dimensionless humidity rate, M_{e} – the equilibrium moisture content, L – the plate thickness. As drying takes place on bottom and top parallel surfaces, L is taken as half of the thickness of the layer. When eq. (12) is applied to materials that dry in long periods such as porous fabrics, the fabric is accepted to be an infinitely thin plate and only the first term on the right side of the equation is taken into consideration. Thus eq. (13) is obtained:

$$MR = \frac{M - M_{\mathrm{e}}}{M_0 - M_{\mathrm{e}}} = \frac{8}{\pi^2} \exp\left[-\frac{\pi^2 D_{\mathrm{eff}} t}{4L^2} \right] \tag{13}$$

The resistance to surface transfer of water vapour is very low in diffusion type drying. Drying rate depends on the diffusion within the material. In this case, the surface moisture content is equal to the equilibrium moisture value M_{e}. This means that the surface moisture content is equal to zero [15].

By taking the equilibrium moisture content M_e to be zero, the dimensionless humidity rate MR provided in eq. (13) can be reduced to the form:

$$MR = \frac{M}{M_0} = \frac{8}{\pi^2}\exp\left[-\frac{\pi^2 D_{\text{eff}} t}{4L^2}\right] \tag{14}$$

The value of the effective diffusion coefficient can be found by converting the expression given in eq. (14) to a logarithmic form, eq. (15), and calculating the slope of the straight line obtained in the graph in which the ln(MR) value is plotted against the drying time:

$$\ln MR = \ln\frac{8}{\pi^2} - \frac{\pi^2 D_{\text{eff}} t}{4L^2} \tag{15}$$

Here, t [s] is the drying time and L [m] – the fabric thickness. In the calculations, half of the fabric thickness was taken, since the drying air was blown from the top and the bottom of the fabric.

In determining of activation energy, the change in effective diffusion coefficient with temperature is explained by an Arrhenius type exponential function [16]:

$$D_{\text{eff}} = D_0 \exp\left(-\frac{E_a}{\text{R}T}\right) \tag{16}$$

where D_{eff} [m^2s^{-1}] is the effective diffusion coefficient, D_0 [m^2s^{-1}] – the constant that is equal to diffusivity at infinite temperature, E_a [kJmol^{-1}] – the activation energy, R – the universal gas constant (8.314 kJ/molK), T [K] – the absolute drying temperature. The slope of the effective diffusion coefficient – temperature graph gives the activation energy [13].

Regression analyses

Microsoft-Excel program was used for the regression analyses. The regression coefficient, R^2, was taken as main criteria in the selection of the equation identifying the drying curves. In addition to the regression coefficient, for the conformity of the utilized model, the values of the mean square deviation chi-square, χ^2, standard error of estimate, *RMSE* and correlation coefficient, r, were also investigated. The mean square deviation values are calculated by using the eq. (17):

$$\chi^2 = \frac{\sum_{i=1}^{n_0}\left(mr_{\text{pre},i} - mr_{\text{exp},i}\right)^2}{n_0 - n_c} \tag{17}$$

Hereby, $mr_{\text{pre},i}$, estimated moisture ratio, $mr_{\text{exp},i}$, the experimental moisture ratio, n_o, number of measurements, n_c expresses the number of parameters in the drying equation nc. Equation (18) is used for standard error of the estimate:

$$RMSE = \sqrt{\frac{\sum_{i=1}^{n_0}\left(mr_{\text{pre},i} - mr_{\text{exp},i}\right)^2}{n_0}} \tag{18}$$

Equation (19) is used for the correlation coefficient calculation.

$$r = \frac{n_0 \sum_{i=1}^{n_0} mr_{\text{pre},i} mr_{\text{exp},i} - \sum_{i=1}^{n_0} mr_{\text{pre},i} \sum_{i=1}^{n_0} mr_{\text{exp},i}}{\sqrt{n_0 \sum_{i=1}^{n_0} \left(mr_{\text{pre},i}\right)^2 - \left(\sum_{i=1}^{n_0} mr_{\text{pre},i}\right)^2} - \sqrt{n_0 \sum_{i=1}^{n_0} \left(mr_{\text{exp},i}\right)^2 - \left(\sum_{i=1}^{n_0} mr_{\text{exp},i}\right)^2}} \tag{19}$$

Results and Discussion

The effect of drying conditions on fabric surface temperature

The change over time in the fabric surface temperature with drying air temperature and fabric movement speed of the drying process can be seen in fig. 7. According to this, it is seen that the surface temperature of 35 °C of the fabric that enters the dryer, depending on the moisture content of the fabric surface, is unable to exceed 84 °C within the first two chambers. Fabric surface temperature, in the later stages of drying especially after chamber sixth, nears the drying air temperature with the effect of the reduced moisture content. Additionally, the decline in the surface temperature of the fabric surface by 9-14 °C between chamber 9 and chamber 10 is due to the heat transfer caused by the opening of the dryer outlet.

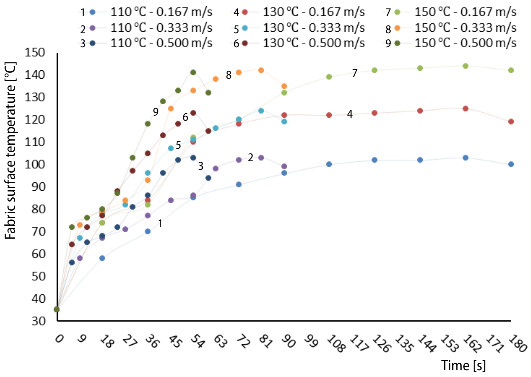

Figure 7. Change in the fabric surface temperature over time

The effect of drying conditions on heat and mass transfer coefficients

When the heat and mass convection coefficients in figs. 8 and 9 are examined, it is seen for the same fabric speed that the heat convection and mass convection coefficients at

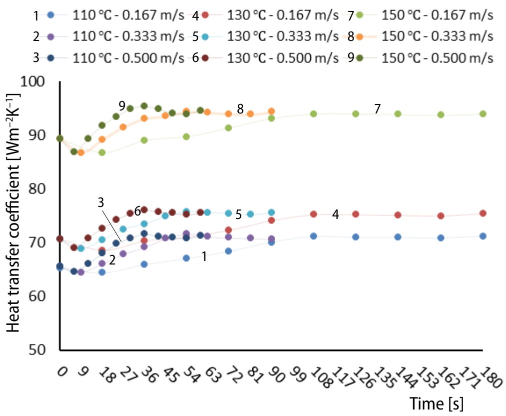

Figure 8. Change of convection heat transfer coefficient over time according to drying conditions

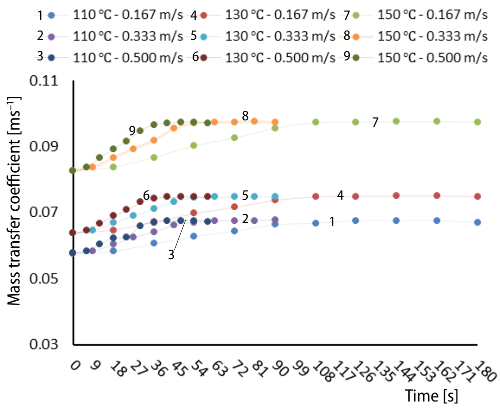

Figure 9. Change of mass transfer coefficient over time according to drying conditions

110 and 130 °C drying air temperature are almost equal, whereas these values increase at the drying air temperature of 150 °C. In parallel to the amount of moisture in the fabric surface, as the fabric surface temperature increases, heat and mass transfer coefficients increase. When the fabric surface temperature approaches the drying air temperature, it is seen that the convection heat transfer coefficient decreases and the mass transfer coefficient remains constant depending on the fabric advancing speed.

The effect of drying conditions on humidity rate and drying rate

From fig. 10, it is seen that the drying rate is highest at 150 °C – 0.167 m/s and lowest at 110 °C – 0.500 m/s drying conditions. The rate of drying is increasing depends on the amount of moisture present on the fabric surface, especially in the first three cabinets. In the later stages of drying, moisture in the fabric is transported to the surface via diffusion and thus evaporated, therefore the drying speed and humidity in the final cabin are about the same. Additionally, at the same fabric feed rate, the drying speed increases with increasing drying air temperature this is due to the fact that the water in the fabric reaching high temperature shows more vapour pressure.

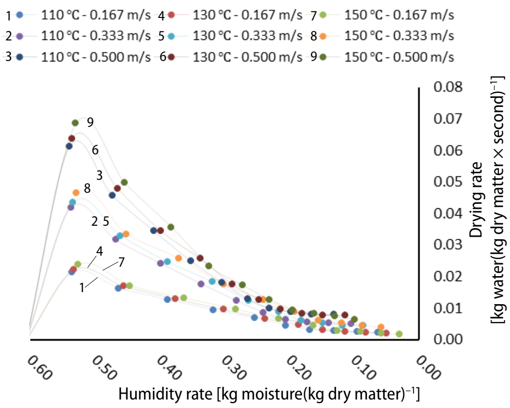

Figure 10. Change in drying rate – humidity rate

Effective diffusion coefficient and activation energy

In the measurements prior to initiating the drying process, the wet fabric weight was measured as 338 g/m^2 and initial moisture, M_o, was determined to be 0.915 kg. Equation (15) was used to determine the effective diffusion coefficient. After the calculation of the lnMR = ln(M/M_o) values, the effective diffusion coefficients found for each case are shown in tab. 6, respectively.

Table 6. Effective diffusion coefficients

Fabric velocity [ms^{-1}]	Drying air temperature [K]	$1/T$ [K^{-1}]	Effective diffusion coefficient D_{eff} [m^{2}s^{-1}]	ln[D_{eff}]
0.167	383	0.00261	1.009 × x 10^{-9}	–20.714
	403	0.00248	1.087 × 10^{-9}	–20.640
	423	0.00236	1.238 × 10^{-9}	–20.510
0.333	383	0.00261	1.676 × 10^{-9}	–20.207
	403	0.00248	1.826 × 10^{-9}	–20.121
	423	0.00236	2.091 × 10^{-9}	–19.986
0.500	383	0.00261	2.247 × 10^{-9}	–19.914
	403	0.00248	2.397 × 10^{-9}	–19.849
	423	0.00236	2.547 × 10^{-9}	–19.788

Activation energy values are calculated by the formula presented in eq. (16) with the help of the graph, fig. 11, that plots ln(D_{eff}) and the reverse of absolute temperature for three different drying air temperatures having the same fabric speed. According to this, activation energy values for fabric speeds of 0.167, 0.333, 0.500 m/s are found to be 6.85, 7.42, and 4.22 kJ/mol, respectively. The increase in effective diffusion coefficient values with increasing drying air temperature can be explained by the easier evaporation of moisture within the products and increase in the drying rate. It is understood from the decreasing activation energy that more moisture diffusion occurs in the drying process with increasing fabric speed.

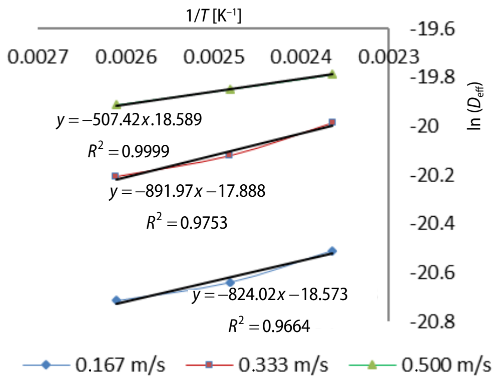

Figure 11 Effect of temperature on effective diffusion coefficient

Regression analyses

The regression analysis values calculated for the model are presented in tab. 7. In model conformity, high R^2 and r values and low χ^2 and *RMSE* values are considered. As it can be seen, for all drying conditions the estimated R^2 values are between 0.9812 and 0.9961, χ^2 values are between 0.00109 and 0.00646, *RMSE* values are between 0.0109 and 0.0289, and r values are between 0.9905 and 0.9980. These values show that the use of the diffusion model as a drying model for the stenter is appropriate.

The change over time in the instantaneous moisture content obtained from the diffusion model and instantaneous moisture content obtained from the studies for all drying conditions have been given in fig. 12.

Table 7. Regression statistics

Fabric velocity [ms^{-1}]	Drying air temperature [K]	R^2	χ^2	*RMSE*	r
0.667	383	0.9881	0.00430	0.0211	0.9940
	403	0.9869	0.00456	0.0228	0.9934
	423	0.9812	0.00646	0.0284	0.9905
0.333	383	0.9941	0.00203	0.0134	0.9970
	403	0.9937	0.00214	0.0146	0.9968
	423	0.9912	0.00322	0.0183	0.9955
0.500	383	0.9949	0.00148	0.0116	0.9974
	403	0.9951	0.00139	0.0120	0.9975
	423	0.9961	0.00109	0.0109	0.9980

Conclusions

In this study, the drying behaviour of a stenter frequently used in the textile industry for drying fabric is determined and modeled. According to the results as follows.

- For all drying conditions, the surface temperature of the fabric that enters the dryer, depending on the moisture content of the fabric surface, is unable to exceed 84 ºC within the first two chambers, and it gets closer to the drying air temperature towards the final chambers due to the reduction in moisture content. It has been observed that the surface temperature of the fabric becomes closer to the drying air temperature in the following stages of the drying process, especially after the 6th cabin, when the amount of free moisture on the surface has disappeared (beginning of the drying phase by diffusion),

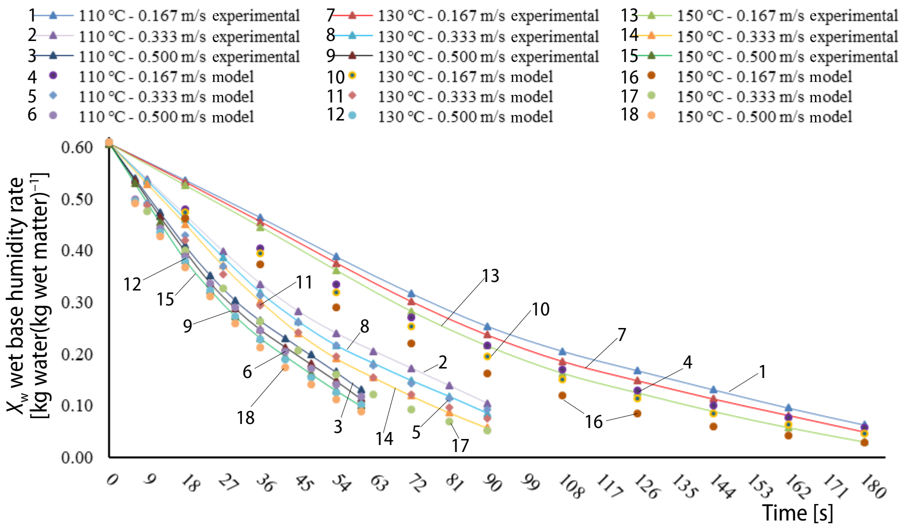

Figure 12. Change over time in model and experimental wet basis moisture content for all drying conditions

- In parallel to the moisture content in the fabric surface, the heat and mass transfer coefficients increase as the fabric surface temperatures increase, while as fabric surface temperature begins to draw closer to the drying air temperature, the convection heat transfer coefficient decreases depending on the fabric speed and the mass transfer coefficient remains the same,
- Drying rate, depending on the moisture content of the fabric surface, is especially higher in the first three chambers in comparison to the other chambers. When the drying air temperature is increased, the amount of evaporation increases. The highest evaporation was obtained at high temperature, at low feed rate. In the variation of the evaporation amount, the drying air temperature was found to be more effective than the fabric speed rate.
- With increasing drying air temperature, the drying speed and the effective diffusion coefficient values increased, and with increasing fabric speed, more moisture diffusing occurred in the drying process, and as a result, the activation energy lowered.
- When the regression statistics are examined, based on the R^2 values ranging between 0.9812 and 0.9961, it is concluded that the use of the diffusion model for the modelling of the drying process in stenters is quite appropriate.

Nomenclature

c_p – specific heat, [kJkg^{-1}K^{-1}]
D_{AB} – mass diffusion coefficient, [m^{2}s^{-1}]
$\varnothing$ – diameter [m]
h – convection heat transfer coefficient, [Wm^{-2}K^{-1}]
h_m – convection mass transfer coefficient, [ms^{-1}]
k – thermal conductivity, [Wm^{-1}K^{-1}]
L – fabric length, [m]
L_c – characteristic length, [m]
Le – Lewis number, (= α/D_{AB}), [–]
M – humidity, [kg]
MR – humidity rate, [mwater mwet^{-1}]
$\dot{m}$ – mass flow, [kgs^{-1}]
Nu – Nusselt number, (= hL/k), [–]
P_g – preassure of gas, [Pa]
Pr – Prandtl number, (= $\mu c_p/k$), [–]
P_v – preassure of water vapour, [Pa]
R – gas constant, [kJkg^{-1}K^{-1}]
R^2 – regression coefficient
RH – relative humidity, (= P_v/P_g at T)
Re – Reynolds number, (= $\rho VLc/\mu$), [–]
Sc – Schimdt number
Sh – Sherwood number, (= $h_m L/D_{AB}$], [–]
T – temperature, [°C or K]
t – time, [s]
V – velocity, [ms^{-1}]

Greek characters

α – thermal diffusion [m^2s^{-1}]
μ – dynamic viscosity [$kgm^{-1}s^{-1}$]
ν – kinematic viscosity [m^2s^{-1}]
ρ – density [kgm^{-3}]

Subscript

a – air
c – characteristic
d – dry
e – equilibrium
f – fabric
s – surface
g – gas
v – vapor
w – water/wet

References

[1] Akyol, U., Theoretical Investigation of Drying of Yarn Coils (in Turkish), Ph. D. thesis, Trakya University, Institute of Science and Technology, Edirne, Turkey, 2007
[2] Sekkeli, M, *et al*., Use of SCADA Software in Textile Factory Paint Plant for Heat Recovery Automation and Application (in Turkish), *Proceedings*, V. Automation Symposium, Izmir, Turkey, 2009
[3] Baxi, H., *et al*., Modelling and Simulation of Dryer System, International Conference on Industrial Instrumentation and Control (ICIC), *Proceedings*, College of Engineering Pune, Pune, India, 2015
[4] Ghali, K., *et al*., Modeling Heat and Mass Transfer in Fabrics, *International Journal of Heat and Mass Transfer, 38* (1995), 1, pp. 13-21
[5] Sousa, L. H. C. D., *et al*., Analysis of Drying Kinetics and Moisture Distribution in Convective Textile Fabric Drying., *Drying Technology, 24* (2006), 4, pp. 485-497
[6] Park, I. S., Baik, D. H., Heat and Mass Transfer Analysis of Fabric in the Tenter Frame, *Textile Research Journal, 67* (1997), 5, pp. 311-316
[7] Etemoglu, A. B., *et al*., Mathematical Modelling of Combined Diffusion of Heat and Mass Transfer Through Fabrics, *Fibers and Polymers, 10*, (2009), 2, pp. 252-259
[8] Johann, G., *et al*., Mathematical Modeling of a Convective Textile Drying Process, *Brazilian Journal of Chemical Engineering, 31*, (2014), 4, pp. 959-965
[9] Alnak, D. E., Karabulut, K., Analysis of Heat and Mass Transfer of The Different Mois Object Geometries with Air Slot Jet Impinging for Forced Convection Drying, *Thermal Science*, *22* (2018), 6B, pp. 2943-2953
[10] Cengel, Y. A., Ghajar, A. J., Heat and Mass Transfer Principles and Applications, *Palme Yayıncılık*, 4th ed., Ankara, 2015
[11] Doymaz, I., (2006). Thin-Layer Drying Behaviour of Mint Leaves, *Journal of Food Engineering, 74* (2006), 3, pp. 370-375
[12] Dincer, A., Experimental Study of Drying Behavior of Yarn Coils and Modeling of Drying, Ph. D. thesis, Trakya Universtiy, Institute of Science and Technology, Edirne, Turkey, 2011
[13] Menges, H. O., Ertekin, C., Study of Thin Layer Drying Characteristics of Carrots, *Agriculture Machines Science Journal, 2* (2006), 4, pp. 353-362
[14] Efremov, G., Kudra, T., Calculation of the Effective Diffusion Coefficients by Applying a Quasi-Stationary Equation for Drying Kinetics, *Drying Technology, 22* (2004), 10, pp. 2273-2279
[15] Geankoplis, C. J., Transfer Processes and Separation Process Principles, (in Turkish) *Guven Kitapevi*, Izmir, Turkey, 2011
[16] Sobukola, O. P., *et al*., Convective Hot Air Drying of Blanched Yam Slices, *International Journal of Food Science and Technology, 43* (2008), 7, pp. 1233-1238

Paper submitted: March 15, 2018
Paper revised: August 10, 2018
Paper accepted: August 14, 2018
© 2020 Society of Thermal Engineers of Serbia
Published by the Vinča Institute of Nuclear Sciences, Belgrade, Serbia.
This is an open access article distributed under the CC BY-NC-ND 4.0 terms and conditions

Appendix 1. Thermodynamic properties of air at film temperature in entry and exit points of the each cabin

Fabric velocity [ms^{-1}]	Time [s]	T_{da} [K]	T_{fs} [K]	T_f [K]	ρ_v [kgm^{-3}]	c_p [kJkg^{-1}K^{-1}]	α [m^{2}s^{-1}]×10^{-7}	D_{AB} [m^{2}s^{-1}] ×10^{-6}	Le [α/D_{AB}]	k [Wm^{-1}K^{-1}] ×10^{-3}	μ [kgm^{-1}s^{-1}]×10^{-6}	ν [m^{2}s^{-1}]×10^{-6}	Pr	V_{da} [ms^{-1}]	Re	Flow type	Nu	Sc	Sh
0.167 - (110 °C)	Entry	383	308	345.5	1.023	1.011	284.759	33.900	0.840	29.446	20.657	20.189	0.709	21.850	1072380	Turb.	2201.386	0.595	2076.502
	18	383	331	357	0.989	1.013	302.462	36.389	0.831	30.283	21.174	21.414	0.708	21.850	1016264	Turb.	2107.745	0.588	1981.763
	36	383	343	363	0.972	1.014	311.465	37.668	0.827	30.698	21.413	22.021	0.707	21.850	1028966	Turb.	2127.792	0.585	1997.145
	54	383	358	370.5	0.951	1.015	323.656	39.408	0.821	31.252	21.771	22.882	0.707	21.850	1027450	Turb.	2125.283	0.581	1990.291
	72	383	364	373.5	0.944	1.015	328.259	40.071	0.819	31.457	21.904	23.208	0.707	21.850	1044111	Turb.	2152.809	0.579	2014.345
	90	383	369	376	0.939	1.016	331.314	40.516	0.818	31.591	21.990	23.424	0.707	21.850	1065936	Turb.	2188.734	0.578	2046.132
	108	383	373	378	0.934	1.016	334.381	40.964	0.816	31.725	22.045	23.607	0.706	21.850	1090454	Turb.	2228.917	0.572	2076.692
	126	383	375	379	0.931	1.016	335.919	41.189	0.816	31.792	22.088	23.716	0.706	21.850	1078869	Turb.	2208.912	0.576	2063.776
	144	383	375	379	0.931	1.016	335.919	41.189	0.816	31.792	22.088	23.716	0.706	21.850	1078869	Turb.	2208.912	0.576	2063.776
	162	383	376	379.5	0.929	1.016	337.461	41.415	0.815	31.859	22.131	23.825	0.706	21.850	1073941	Turb.	2200.836	0.575	2055.627
	180	383	373	378	0.934	1.016	334.381	40.964	0.816	31.725	22.045	23.607	0.706	21.850	1092319	Turb.	2231.967	0.572	2079.534
	Exit	383	341	362	0.975	1.013	309.956	37.453	0.828	30.629	21.399	21.945	0.708	21.850	1165935	Turb.	2352.623	0.586	2208.805
0.167 - (130 °C)	Entry	403	308	355.5	0.994	1.012	299.488	35.968	0.833	30.144	21.084	21.204	0.708	24.450	1142818	Turb.	2315.232	0.589	2177.485
	18	403	347	375	0.941	1.016	329.785	40.293	0.818	31.524	21.947	23.316	0.707	24.450	1044451	Turb.	2153.370	0.579	2014.269
	36	403	357	380	0.929	1.016	337.461	41.415	0.815	31.859	22.131	23.825	0.706	24.450	1064216	Turb.	2184.877	0.575	2040.721
	54	403	383	393	0.898	1.018	357.789	44.404	0.806	32.730	22.688	25.260	0.706	24.450	1041500	Turb.	2147.488	0.569	1998.322
	72	403	391	397	0.889	1.019	364.151	45.346	0.803	32.998	22.859	25.709	0.706	24.450	1054688	Turb.	2169.214	0.567	2016.282
	90	403	395	399	0.885	1.019	367.351	45.820	0.802	33.132	22.944	25.935	0.706	24.450	1082268	Turb.	2214.476	0.566	2057.212
	108	403	395	399	0.885	1.019	367.351	45.820	0.802	33.132	22.944	25.935	0.706	24.450	1102065	Turb.	2246.825	0.566	2087.263
	126	403	396	399.5	0.882	1.020	368.956	46.059	0.801	33.199	22.987	26.048	0.706	24.450	1099150	Turb.	2242.068	0.566	2082.269
	144	403	397	400	0.880	1.020	370.564	46.297	0.800	33.266	23.029	26.162	0.706	24.450	1094381	Turb.	2234.282	0.565	2074.467
	162	403	398	400.5	0.878	1.020	372.174	46.537	0.800	33.333	23.072	26.276	0.706	24.450	1089644	Turb.	2226.542	0.565	2066.714
	180	403	392	397.5	0.887	1.019	365.750	45.583	0.802	33.065	22.902	25.822	0.706	24.450	1108785	Turb.	2257.777	0.566	2098.018
	Exit	403	366	384.5	0.917	1.017	345.216	42.552	0.811	32.194	22.346	24.372	0.706	24.450	1174735	Turb.	2364.587	0.573	2205.364
0.167- (150 °C)	Entry	423	308	365.5	0.964	1.014	316.012	38.315	0.825	30.906	21.548	22.342	0.707	33.400	1488960	Turb.	2859.661	0.583	2681.787
	18	423	347	385	0.917	1.017	345.216	42.552	0.811	32.194	22.346	24.372	0.706	33.400	1364929	Turb.	2666.192	0.573	2486.659
	36	423	355	389	0.907	1.018	351.477	43.473	0.809	32.462	22.517	24.814	0.706	33.400	1395800	Turb.	2714.325	0.571	2528.649
	54	423	385	404	0.874	1.020	375.406	47.018	0.798	33.467	23.124	26.466	0.705	33.400	1357903	Turb.	2653.952	0.563	2462.099
	72	423	393	408	0.865	1.021	381.906	47.988	0.796	33.735	23.294	26.924	0.705	33.400	1375729	Turb.	2681.787	0.561	2485.230
	90	423	405	414	0.853	1.022	391.749	49.461	0.792	34.137	23.548	27.618	0.705	33.400	1388326	Turb.	2701.414	0.558	2499.415
	108	423	412	417.5	0.846	1.023	396.713	50.207	0.790	34.338	23.675	27.968	0.705	33.400	1390214	Turb.	2704.354	0.557	2499.504
	126	423	415	419	0.842	1.023	400.037	50.707	0.789	34.472	23.759	28.203	0.705	33.400	1386801	Turb.	2699.040	0.556	2493.942
	144	423	416	419.5	0.840	1.023	401.704	50.958	0.788	34.539	23.802	28.320	0.705	33.400	1381046	Turb.	2690.076	0.556	2485.013
	162	423	417	420	0.838	1.023	403.374	51.210	0.788	34.606	23.844	28.438	0.705	33.400	1375328	Turb.	2681.163	0.555	2476.136
	180	423	415	419	0.842	1.023	400.037	50.707	0.789	34.472	23.759	28.203	0.705	33.400	1386801	Turb.	2699.040	0.556	2493.942
	Exit	423	384	403.5	0.874	1.020	375.406	47.018	0.798	33.467	23.124	26.466	0.705	33.400	1477792	Turb.	2839.807	0.563	2634.518

→

Appendix 1. (Continuation)

Fabric velocity [ms^{-1}]	Time [s]	T_{da} [K]	T_{fs} [K]	T_f [K]	ρ_v [kgm^{-3}]	c_p [kJkg^{-1}K^{-1}]	α [m^{2}s^{-1}]×10^{-7}	D_{AB} [m^{2}s^{-1}] ×10^{-6}	Le [α/D_{AB}]	k [Wm^{-1}K^{-1}] ×10^{-3}	μ [kgm^{-1}s^{-1}]×10^{-6}	ν [m^{2}s^{-1}]×10^{-6}	Pr	V_{da} [ms^{-1}]	Re	Flow type	Nu	Sc	Sh
0.3333 - (110 °C)	Entry	383	308	345.5	1.023	1.011	284.759	33.900	0.840	29.446	20.657	20.189	0.709	21.850	1072380	Turb.	2201.386	0.595	2076.502
	9	383	331	357	0.989	1.013	302.462	36.389	0.831	30.283	21.174	21.414	0.708	21.850	1016264	Turb.	2107.745	0.588	1981.763
	18	383	340	361.5	0.978	1.013	308.451	37.239	0.828	30.560	21.354	21.838	0.708	21.850	1032515	Turb.	2134.666	0.586	2004.171
	27	383	344	363.5	0.970	1.014	312.977	37.883	0.826	30.767	21.458	22.128	0.707	21.850	1062506	Turb.	2183.098	0.584	2048.470
	36	383	350	366.5	0.962	1.014	317.534	38.533	0.824	30.975	21.592	22.450	0.707	21.850	1079377	Turb.	2210.787	0.583	2072.687
	45	383	357	370	0.954	1.015	322.121	39.188	0.822	31.182	21.727	22.774	0.707	21.850	1101427	Turb.	2246.843	0.581	2104.716
	54	383	359	371	0.951	1.015	323.656	39.408	0.821	31.252	21.771	22.882	0.707	21.850	1116254	Turb.	2271.007	0.581	2126.759
	63	383	371	377	0.936	1.016	332.846	40.740	0.817	31.658	22.033	23.532	0.707	21.850	1087292	Turb.	2223.745	0.578	2078.862
	72	383	375	379	0.931	1.016	335.919	41.189	0.816	31.792	22.088	23.716	0.706	21.850	1078869	Turb.	2208.912	0.576	2063.776
	81	383	376	379.5	0.929	1.016	337.461	41.415	0.815	31.859	22.131	23.825	0.706	21.850	1073941	Turb.	2200.836	0.575	2055.627
	90	383	375	379	0.926	1.016	339.005	41.641	0.814	31.926	22.174	23.934	0.706	21.850	1078869	Turb.	2208.912	0.576	2063.776
	Exit	383	358	370.5	0.954	1.015	322.121	39.188	0.822	31.182	21.727	22.774	0.707	21.850	1118164	Turb.	2274.115	0.581	2129.669
0.333 - (130 °C)	Entry	403	308	355.5	0.992	1.012	300.973	36.178	0.832	30.214	21.129	21.309	0.708	24.450	1142818	Turb.	2315.232	0.589	2177.485
	9	403	340	371.5	0.949	1.015	325.195	39.628	0.821	31.321	21.816	22.991	0.707	24.450	1059193	Turb.	2177.652	0.580	2038.766
	18	403	351	377	0.936	1.016	332.846	40.740	0.817	31.658	22.033	23.532	0.707	24.450	1077445	Turb.	2207.621	0.578	2063.788
	27	403	355	379	0.931	1.016	335.919	41.189	0.816	31.792	22.088	23.716	0.706	24.450	1109307	Turb.	2258.627	0.576	2110.225
	36	403	369	386	0.914	1.017	346.777	42.781	0.811	32.261	22.389	24.482	0.706	24.450	1107531	Turb.	2255.735	0.572	2103.235
	45	403	380	391.5	0.900	1.018	356.206	44.170	0.806	32.663	22.645	25.148	0.706	24.450	1116129	Turb.	2269.733	0.569	2112.671
	54	403	384	393.5	0.896	1.019	359.375	44.639	0.805	32.797	22.731	25.372	0.706	24.450	1126525	Turb.	2286.631	0.568	2127.202
	63	403	389	396	0.891	1.019	362.556	45.109	0.804	32.931	22.816	25.596	0.706	24.450	1118552	Turb.	2273.674	0.567	2113.965
	72	403	393	398	0.887	1.019	365.750	45.583	0.802	33.065	22.902	25.822	0.706	24.450	1108785	Turb.	2257.777	0.566	2098.018
	81	403	397	400	0.882	1.020	368.956	46.059	0.801	33.199	22.987	26.048	0.706	24.450	1099150	Turb.	2242.068	0.566	2082.269
	90	403	392	397.5	0.887	1.019	365.750	45.583	0.802	33.065	22.902	25.822	0.706	24.450	1113652	Turb.	2265.702	0.567	2105.967
	Exit	403	373	388	0.910	1.018	349.907	43.242	0.809	32.395	22.474	24.703	0.706	24.450	1158986	Turb.	2339.192	0.571	2179.799
0.333 - (150 °C)	Entry	423	308	365.5	0.964	1.014	316.012	38.315	0.825	30.906	21.548	22.342	0.707	33.400	1488960	Turb.	2859.661	0.583	2681.787
	9	423	346	384.5	0.917	1.017	345.216	42.552	0.811	32.194	22.346	24.372	0.706	33.400	1364929	Turb.	2666.192	0.573	2486.659
	18	423	352	387.5	0.910	1.018	349.907	43.242	0.809	32.395	22.474	24.703	0.706	33.400	1402063	Turb.	2724.064	0.571	2538.447
	27	423	357	390	0.905	1.018	353.050	43.705	0.808	32.529	22.560	24.925	0.706	33.400	1441840	Turb.	2785.717	0.570	2594.419
	36	423	366	394.5	0.894	1.019	360.964	44.874	0.804	32.864	22.774	25.484	0.706	33.400	1453482	Turb.	2803.696	0.568	2607.486
	45	423	398	410.5	0.859	1.022	386.813	48.722	0.794	33.936	23.421	27.270	0.705	33.400	1406041	Turb.	2728.955	0.560	2526.909
	54	423	406	414.5	0.851	1.022	393.400	49.709	0.791	34.204	23.590	27.735	0.705	33.400	1407787	Turb.	2731.667	0.558	2526.738
	63	423	411	417	0.846	1.023	396.713	50.207	0.790	34.338	23.675	27.968	0.705	33.400	1398422	Turb.	2717.120	0.557	2511.961
	72	423	414	418.5	0.842	1.023	400.037	50.707	0.789	34.472	23.759	28.203	0.705	33.400	1386801	Turb.	2699.040	0.556	2493.942
	81	423	415	419	0.840	1.023	401.704	50.958	0.788	34.539	23.802	28.320	0.705	33.400	1381046	Turb.	2690.076	0.556	2485.013
	90	423	408	415.5	0.849	1.022	395.055	49.958	0.791	34.271	23.633	27.851	0.705	33.400	1404290	Turb.	2726.237	0.557	2521.051
	Exit	423	386	404.5	0.872	1.020	377.026	47.259	0.798	33.534	23.167	26.580	0.705	33.400	1471441	Turb.	2830.039	0.562	2624.743

→

Appendix 1. (Continuation)

Fabric velocity [ms^{-1}]	Time [s]	T_{da} [K]	T_{fs} [K]	T_f [K]	ρ_v [kgm^{-3}]	c_p [kJkg^{-1}K^{-1}]	α [m^{2}s^{-1}]×10^{-7}	D_{AB} [m^{2}s^{-1}] ×10^{-6}	Le [α/D_{AB}]	k [Wm^{-1}K^{-1}] ×10^{-3}	μ [kgm^{-1}s^{-1}]×10^{-6}	ν [m^{2}s^{-1}]×10^{-6}	Pr	V_{da} [ms^{-1}]	Re	Flow type	Nu	Sc	Sh
0.500 - (110 °C)	Entry	383	308	345.5	1.020	1.011	286.230	34.104	0.839	29.518	20.704	20.294	0.709	21.850	1072380	Turb.	2201.386	0.595	2076.502
	6	383	329	356	0.992	1.012	300.973	36.178	0.832	30.214	21.129	21.309	0.708	21.850	1021291	Turb.	2116.082	0.589	1990.184
	12	383	338	360.5	0.978	1.013	308.451	37.239	0.828	30.560	21.354	21.838	0.708	21.850	1037555	Turb.	2142.997	0.586	2012.572
	18	383	341	362	0.975	1.013	309.956	37.453	0.828	30.629	21.399	21.945	0.708	21.850	1071346	Turb.	2198.653	0.586	2064.247
	24	383	345	364	0.970	1.014	312.977	37.883	0.826	30.767	21.458	22.128	0.707	21.850	1062506	Turb.	2183.098	0.584	2048.470
	30	383	354	368.5	0.957	1.015	320.588	38.969	0.823	31.113	21.682	22.666	0.707	21.850	1106690	Turb.	2255.429	0.582	2113.351
	36	383	359	371	0.951	1.015	323.656	39.408	0.821	31.252	21.771	22.882	0.707	21.850	1116254	Turb.	2271.007	0.581	2126.759
	42	383	369	376	0.939	1.016	331.314	40.516	0.818	31.591	21.990	23.424	0.707	21.850	1087292	Turb.	2223.745	0.578	2078.862
	48	383	375	379	0.931	1.016	335.919	41.189	0.816	31.792	22.088	23.716	0.706	21.850	1078869	Turb.	2208.912	0.576	2063.776
	54	383	376	379.5	0.929	1.016	337.461	41.415	0.815	31.859	22.131	23.825	0.706	21.850	1073941	Turb.	2200.836	0.575	2055.627
	60	383	367	375	0.941	1.016	329.785	40.293	0.818	31.524	21.947	23.316	0.707	21.850	1097383	Turb.	2240.241	0.579	2095.528
	Exit	383	362	372.5	0.946	1.015	326.737	39.849	0.820	31.390	21.861	23.100	0.707	21.850	1107620	Turb.	2256.945	0.580	2112.416
0.500 - (130 °C)	Entry	403	308	355.5	0.992	1.012	300.973	36.178	0.832	30.214	21.129	21.309	0.708	24.450	1142818	Turb.	2315.232	0.589	2177.485
	6	403	337	370	0.954	1.015	322.121	39.188	0.822	31.182	21.727	22.774	0.707	24.450	1069302	Turb.	2194.262	0.581	2055.462
	12	403	345	374	0.944	1.015	328.259	40.071	0.819	31.457	21.904	23.208	0.707	24.450	1092500	Turb.	2232.262	0.579	2088.688
	18	403	350	376.5	0.936	1.016	332.846	40.740	0.817	31.658	22.033	23.532	0.707	24.450	1117967	Turb.	2273.795	0.578	2125.651
	24	403	361	382	0.924	1.017	340.553	41.867	0.813	31.993	22.217	24.043	0.706	24.450	1127770	Turb.	2288.652	0.574	2136.400
	30	403	370	386.5	0.912	1.017	348.340	43.011	0.810	32.328	22.431	24.593	0.706	24.450	1141333	Turb.	2310.644	0.572	2153.814
	36	403	378	390.5	0.903	1.018	354.627	43.937	0.807	32.596	22.603	25.037	0.706	24.450	1141608	Turb.	2311.090	0.570	2151.775
	42	403	386	394.5	0.894	1.019	360.964	44.874	0.804	32.864	22.774	25.484	0.706	24.450	1123485	Turb.	2281.693	0.568	2122.014
	48	403	391	397	0.889	1.019	364.151	45.346	0.803	32.998	22.859	25.709	0.706	24.450	1113652	Turb.	2265.702	0.567	2105.967
	54	403	396	399.5	0.882	1.020	368.956	46.059	0.801	33.199	22.987	26.048	0.706	24.450	1099150	Turb.	2242.068	0.566	2082.269
	60	403	388	395.5	0.882	1.020	368.956	46.059	0.801	33.199	22.987	26.048	0.706	24.450	1118552	Turb.	2273.674	0.567	2113.965
	Exit	403	385	394	0.896	1.019	359.375	44.639	0.805	32.797	22.731	25.372	0.706	24.450	1128453	Turb.	2289.760	0.568	2130.113
0.500 - (150 °C)	Entry	423	308	365.5	0.964	1.014	316.012	38.315	0.825	30.906	21.548	22.342	0.707	33.400	1488960	Turb.	2859.661	0.583	2681.787
	6	423	345	384	0.919	1.017	343.659	42.323	0.812	32.127	22.303	24.262	0.706	33.400	1371115	Turb.	2675.854	0.573	2496.392
	12	423	349	386	0.914	1.017	346.777	42.781	0.811	32.261	22.389	24.482	0.706	33.400	1414721	Turb.	2743.721	0.572	2558.230
	18	423	353	388	0.910	1.018	349.907	43.242	0.809	32.395	22.474	24.703	0.706	33.400	1454793	Turb.	2805.719	0.571	2614.537
	24	423	360	391.5	0.900	1.018	356.206	44.170	0.806	32.663	22.645	25.148	0.706	33.400	1472894	Turb.	2833.613	0.569	2637.532
	30	423	376	399.5	0.882	1.020	368.956	46.059	0.801	33.199	22.987	26.048	0.706	33.400	1472005	Turb.	2832.245	0.566	2630.383
	36	423	391	407	0.867	1.021	380.276	47.744	0.796	33.668	23.252	26.809	0.705	33.400	1456374	Turb.	2806.832	0.562	2601.811
	42	423	401	412	0.857	1.022	388.455	48.968	0.793	34.003	23.463	27.386	0.705	33.400	1428148	Turb.	2763.227	0.559	2557.962
	48	423	413	418	0.844	1.023	398.373	50.457	0.790	34.405	23.717	28.085	0.705	33.400	1392593	Turb.	2708.054	0.557	2502.925
	54	423	414	418.5	0.842	1.023	400.037	50.707	0.789	34.472	23.759	28.203	0.705	33.400	1386801	Turb.	2699.040	0.556	2493.942
	60	423	405	414	0.853	1.022	391.749	49.461	0.792	34.137	23.548	27.618	0.705	33.400	1416141	Turb.	2744.626	0.558	2539.396
	Exit	423	393	408	0.865	1.021	381.906	47.988	0.796	33.735	23.294	26.924	0.705	33.400	1452641	Turb.	2801.074	0.561	2595.774